Energy, Mines and Resources Canada | Énergie, Mines et Ressources Canada

CANMET

Canada Centre for Mineral and Energy Technology | Centre canadien de la technologie des minéraux et de l'énergie

CHARACTERIZATION OF GRANULATED BLAST FURNACE SLAG FOR PORTLAND CEMENT REPLACEMENT IN CONCRETE

E. Douglas
Mineral Processing Laboratory
R.T. Hemmings
Ontario Research Foundation

May 1986

Project: 3.0.3.7.01
Energy Research and Development

This work was supported by the Federal Panel on Energy R&D (PERD).

This document is an unedited interim report prepared primarily for ... and internal ... purposes. It does not represent a final expression of the opinion of the Canada Centre for Mineral and Energy Technology (CANMET)

Ce document est un rapport ... provisoire non-révisé et rédigé ... principalement pour ... de documentation ... ne représente nulle... l'opinion définitive de ... du Centre canadien de la technologie des minéraux et de l'énergie (CANMET)

45 pp

MINERAL SCIENCES LABORATORIES
DIVISION REPORT MSL 86-67 (IR)

AUG 19 1986
MICROMEDIA

CHARACTERIZATION OF GRANULATED BLAST FURNACE SLAG FOR PORTLAND CEMENT REPLACEMENT IN CONCRETE

by

E. Douglas* and R.T. Hemmings**

ABSTRACT

A Canadian granulated blast furnace slag from a new source (Sault Ste. Marie, Ontario), was ground in the laboratory to 4000 and 5000 cm^2/g. The slags were characterized by a range of techniques including particle size analysis, specific gravity, chemical analysis, scanning electron microscope-energy dispersive X-ray analysis, and X-ray powder diffractometry. It was found that the slag was highly vitreous and could be identified as a calcium magnesium aluminosilicate glass with melilite as the minor crystalline component. Free MgO was not detected. Slag activity indices for the two grades were determined as mortars (50:50) at 7 and 28 d. All the slag-cement mortars had lower early strengths than the control OPC mortar; however, at 28 d, the 4000 and 5000 cm^2/g slag-cement mortars exceeded the control. The hydration of slag-cement pastes (50:50 and 70:30) was investigated at W/C = 0.5 and curing ages from 2 h to 28 d by following the chemical composition of expressed pore fluids and by determining the $Ca(OH)_2$ and chemically bound water by their thermogravimetric analysis. Phase composition by XRD and microstructural features were determined as well. In the early stages of hydration, Ca^{2+} and SO_4^{2-} are present in the pore fluids but, compared to a control of OPC paste, they are mobilized at different rates to form insoluble ettringite. The slag does not appear to contribute significantly to the pore fluid ions at 28 d. Thermal analysis indicates that $Ca(OH)_2$ is probably not formed by hydration

---

*Research Scientist, Construction Materials Section, CANMET, Energy, Mines and Resources Canada.

**Project Manager, Materials Division, Industrial Materials Centre, Ontario Research Foundation.

of the slag. However, the non-evaporable water contents of the paste confirm the hydraulic nature of the slags. Further work to identify the hydration phases is needed as part of an evaluation of the long term durability of the binder.

CARACTÉRISATION DU LAITIER GRANULÉ DE HAUT-FOURNEAU COMME PRODUIT DE REMPLACEMENT DU CIMENT PORTLAND DANS LE BÉTON

par

E. Douglas* et R.T. Hemmings**

RÉSUMÉ

Un laitier granulé canadien de haut-fourneau provenant d'une nouvelle source (Sault Ste. Marie, Ontario) a été broyé en laboratoire à 4000 et 5000 cm^2/g. Les laitiers ont été caractérisés au moyen d'une gamme de techniques y compris des analyses granulométrique, de densité, chimique, et des analyses par microscopie à balayage électronique par dipersion des rayons X et par diffraction des rayons X par des poudres. On a découvert que le laitier était très vitreux et pouvait être identifié comme du verre d'alumino-silicate magnésien-calcique dont le constituant cristallin mineur est la mélilite. On n'a pas détecté de MgO libre. Les indices de l'activité du laitier pour les deux classes ont été déterminés en tant que mortiers (50:50) à 7 et 28 j. Tous les mortiers composés de laitier et de ciment avaient une résistance première moins élevée que le mortier de contrôle OPC; cependant, à 28 j., la résistance des mortiers de 4000 et 5000 cm^2/g, composés de laitier et de ciment, était supérieure à celle du mortier servant au contrôle. L'hydratation des pâtes composées de laitier et de ciment (50:50 et 70-30) a été investiguée à W/C = 0,5 et un temps de prise de 2 à 28 j. en suivant la composition chimique des fluides des pores et en déterminant le $Ca(OH)_2$ et l'eau limitée chimiquement au moyen d'une analyse thermogravimétrique. On a également déterminé les caractéristiques microstructurales et la composition de la phase par diffraction de rayons X. Dans les phases premières de l'hydratation, Ca^{2+} et SO^{2-} sont présents dans les fluides des pores mais, comparativement à la pâte de contrôle OPC, ils sont mobilisés

---

*Chercheur scientifique, Section des matériaux de construction, CANMET, Énergie, Mines et Ressources Canada.

**Chef de projet, Division des matériaux, Centre industriel des matériaux Fondation de recherche de l'Ontario.

dans divers rapports pour former de l'éttringite insoluble. À 28 j., le laitier ne semble pas contribuer de façon importante à la formation d'ions dans le fluide des pores. L'analyse thermique indique que $Ca(OH)_2$ n'est probablement pas formé par l'hydratation du laitier. Cependant, la teneur en eau non évaporable de la pâte confirme la nature hydraulique des laitiers. Des études plus poussées en vue d'identifier les phases d'hydratation sont nécessaires dans le cadre de l'évaluation de la durabilité à long terme du liant.

CONTENTS

	Page
ABSTRACT	i
RÉSUMÉ	iii
INTRODUCTION	1
EXPERIMENTAL METHODS	1
MATERIALS	1
CHARACTERIZATION OF SLAGS	2
1. Particle size analysis	2
2. Specific gravity	2
3. Chemical analysis	2
4. Glass content and mineralogy	3
a) Optical method	3
b) QXRD method	3
5. Slag activity indices	3
6. Analysis of hydration products of portland cement-slag pastes	3
a) Pore fluid expression and analysis	3
b) Thermal analysis of pastes	4
c) X-ray diffraction analysis of pastes	4
d) Scanning electron microscopy of pastes	5
RESULTS AND DISCUSSION	5
SLAG CHARACTERISTICS	5
PORTLAND CEMENT-SLAG HYDRATION	6
Pore fluid chemistry	6
Phase identification and microstructure of pastes	10
SUMMARY AND CONCLUSIONS	12
ACKNOWLEDGEMENTS	13
REFERENCES	13

TABLES

No.		
1.	Chemical and physical characteristics of portland cement	16
2.	Specific gravities and particle size analysis of laboratory ground blast furnace slags	17

TABLES (Cont'd)

No.		Page
3.	Chemical analysis data for slags	18
4.	Slag activity index data for OPC-BFS mortars	19
5.	Air content of mortars	20
6.	Chemical data for pore fluid extracted from slag-cement pastes (50% w/w slag)	21
7.	Chemical data for pore water extracted from slag-cement pastes (70% w/w slag)	22
8.	Chemical data for pore fluid normalized to initial volume of water (50% w/w slag)	23
9.	Chemical data for pore fluids normalized to initial volume of water (70% w/w slag)	24
10.	TGA/DTG data for OPC-BFS pastes (50% replacement)	25
11.	TGA/DTG data for OPC-BFS pastes (70% replacement)	26

FIGURES

1.	Particle size distribution of 4000 and 5000 cm^2/g slags	27
2.	XRD traces showing identification of principal phases in OPC-BFS pastes (50:50)	28
3a.	Scanning electron micrographs of control OPC paste at 5 h	29
3b.	Scanning electron micrographs of control OPC paste at 7 d	30
4a.	Scanning electron micrographs of 4000 cm^2/g slag cement paste at 5 h	31
4b.	Scanning electron micrographs of 4000 cm^2/g slag cement paste at 7 d	32
5.	XRD traces (CuKα) for slags	33
6.	Location of slag composition in idealized $CaO-SiO_2-MgO$ phase system (10% Al_2O_3)	34
7.	Uncorrected variation in concentration of principal pore fluid ions expressed from OPC-BFS pastes (50:50 and 30:70) at curing ages up to 28 d	35
8.	Variation in concentration of principal pore fluid ions expressed from OPC-BFS pastes (50:50 and 30:70) at curing ages up to 28 d (Data normalized to initial H_2O volume)	36

FIGURES (Cont'd)

No.		Page
9.	Calcium hydroxide content of portland cement-slag pastes in g/100 g total binder	37
10.	Non-evaporable water content in g/100 g total binder, of portland cement-slag pastes	37

INTRODUCTION

The increased availability of blast furnace slag for the construction industry offers opportunities for the design and manufacture of concrete with higher durability than concrete with portland cement alone. To compare the performance of blast furnace slags it is necessary to characterize and evaluate the performance of the slags in mortar and concrete mixes. The present study concerns the behaviour of a new source of granulated blast furnace slag from Sault Ste. Marie, Ontario, to be used as a partial replacement for portland cement in concrete.

The scope and objectives of the work are summarized as follows:

1. Characterization of blast furnace slag raw materials ground in the laboratory to 4000 and 5000 cm^2/g by particle size analysis, specific gravity, chemical analysis, morphology by scanning electron microscopy, glass content and mineralogy by optical microscopy and X-ray powder diffractometry.
2. Determination of 7 d and 28 d slag activity indices (ASTM C 989) for 4000 and 5000 cm^2/g slags in OPC-BFS mortars of 50:50 w/w mixes.
3. Investigation of the hydration behaviour of OPC-BFS pastes in 50:50 and 30:70 w/w mixes, by following the chemistry of expressed pore fluids and monitoring TGA/DTG-derived $Ca(OH)_2$ and non-evaporable water contents of the solid phase of pastes at curing ages up to 28 days.
4. Observation of morphological and mineralogical features in the hydrating pastes by scanning electron microscopy-energy dispersive X-ray analysis (SEM-EDXD) and X-ray diffraction (XRD).

EXPERIMENTAL METHODS

MATERIALS

The developmental blast furnace slag originated from pilot scale granulation trials carried out at the steel mill (Sault Ste. Marie). Slags ground to 3400 and 4800 cm^2/g were reground in the laboratory by dry ball-milling to provide two grades with nominal finenesses of 4000 and 5000 (±100) cm^2/g (Blaine).

The cement used throughout the study for the preparation of pastes and mortars was a CSA Type 10 portland cement. The chemical and physical characteristics of the cement are given in Table 1. Chemically the cement conforms to the requirements of ASTM C 989 for total alkali content, i.e., alkalies <0.9% as Na_2O.

The water used for the hydration of the pastes and mortars was of deionized laboratory grade which had been boiled to remove CO_2. The pH of the water was 6.9-7.1 with the following trace element content: S<0.05; Al<0.02; Fe<0.02; Ca<0.02; Mg<0.02; Na<0.5; K<0.1 $\mu g.mL^{-1}$.

Characterization of Slags

1. Particle size analysis

The particle size distribution and statistics for the materials were determined by the electrozone technique (TA II Coulter counter) using a conventional multi-tube overlap method with 280, 70 and 30 µm tubes for an effective particle size analyzing range of 0.63 to 128 µm. The particle size statistics by volume for the slags are given in Table 2. Cumulative particle size distributions by volume for the 4000 and 5000 cm^2/g slags are given in Fig. 1.

2. Specific gravity

The specific gravities of the slags were determined by the Le Chatelier method using alcohol as the fluid displacement medium and were as follows: 4000 cm^2/g 2.86; 5000 cm^2/g 2.88. The two materials had a specific gravity (true particle density) of 2.92 by air comparison pycrometry (ASTM D 2840).

3. Chemical analysis

Chemical analysis of the slags, dried at 110°C, for major and minor elements was carried out by inductively coupled argon plasma (ICAP) spectroscopy. Total sulphur was determined by LECO analyzer. The analytical results are given conventionally in terms of the element oxide in Table 3.

4. Glass content and mineralogy

a) Optical method

The glass content of the 4000 cm^2/g slag was determined according to the modified McMaster optical technique (1) using a transmitted light, polarizing microscope with a removable gypsum plate. No magnetic material was apparent on treating the samples with a hand magnet. By this method, the glass content of the 4000 cm^2/g materials was determined to be 95% by duplicate determinations.

b) QXRD method

Quantitative X-ray diffraction analysis of the slags was carried out on an automated diffractometer using monochromatic CuKα radiation with 40 kV and 40 mA. Routine scans of the two slags are shown in Fig. 2. Aside from the predominantly glassy nature of the materials, as indicated by the broad diffraction maxima extending from 20-40°2θ and centered at approximately 32°2θ, the small quantity of crystalline scattering is identified as melilite, a solid solution in the gehlenite-akermanite (C_2AS-C_2MS_2) series. The glass content in the slag was determined by a QXRD method (2) using reference curves for melilite and an internal CaF_2 standard. Measured glass content values for the 4000 and 5000 cm^2/g slags were 89.5 and 90.9% respectively, by triplicate determinations.

5. Slag activity indices

Slag activity indices for 4000 and 5000 cm^2/g materials were determined at 7 and 28 d for OPC-BFS (50:50) mortars according to the procedures specified in ASTM C 989-82. Corresponding air contents were determined according to ASTM C 185. The results are shown in Tables 4 and 5.

6. Analysis of hydration products of portland cement-slag pastes

a) Pore fluid expression and analysis

A series of OPC-BFS pastes was prepared at water/binder ratio of 0.50 at OPC replacement levels of 50 and 70% w/w for each of the 4000 and 5000 cm^2/g slags. A control paste with 100% OPC was prepared for reference purposes. Exposure to air was controlled during the preparation and handling

of the pastes to minimize carbonation effects. All pastes were sealed in plastic molds (2.5 cm diam x 5 cm height) and cured at 21 (±1)°C until time of test.

At curing ages of 2 h, 5 h, 1 d, 3 d, 7 d and 28 d the pore fluid was expressed from the pastes using a high pressure technique based on earlier work by Longuet (3) and Barneyback and Diamond (4). A nitrogen blanket was maintained in the apparatus during the expression and manipulation to prevent carbonation of the highly alkaline fluids. The resultant fluid was immediately diluted to standard volume and analyzed: for Si, Fe, Ca, Al, Na and K by DC plasma spectrophotometry; for SO_4^{2-} by ion chromatography, and pH by titration with standard HCl to the methyl red end point.

The results of the pore fluid analysis are given in an uncorrected form for the pastes with 50% and 70% slag in Tables 6 and 7, respectively. Correlated data which have been normalized to the initial volume of water are given in Tables 8 and 9, using TGA-derived bound water contents, following the general approach of Diamond (5).

b) Thermal analysis of pastes

Immediately following the expression of pore fluids, samples for thermal analysis were recovered from the solid paste residues and ground in dry acetone (2 cycles) to arrest further hydration. This was followed by drying to constant weight at 60°C in dry nitrogen, a procedure which has been shown to closely simulate d-drying conditions (6). After drying, all storage and sample manipulation was carried out in a dry CO_2-free nitrogen atmosphere. A background correction factor was first determined from the thermal curve of unhydrated OPC. This factor was then used to generate corrected and normalized calcium hydroxide and non-evaporable water contents (Tables 10 and 11). For comparison purposes, the data are expressed in terms of grams per 100 g OPC and grams per 100 g total binder for both 50 and 70% replacement levels.

c) X-ray diffraction analysis of pastes

Limited qualitative XRD analysis was carried out to assist in the identification of hydration products present in the OPC-BFS pastes. For this purpose an OPC-BFS (50:50) paste was prepared at w/c = 0.50. After curing ages of 1 d, 3 d, 7 d and 28 d and drying by the above mentioned technique, specimens were ground and examined by XRD. Major phases identified in the XRD traces are shown in Fig. 2.

d) Scanning electron microscopy of pastes

The development of paste microstructure and hydration products was monitored by SEM-EDXA on the following specimens prepared as described above at curing ages of 5 h and 7 d: control, 100% OPC and 50% 4000 cm^2/g OPC-BFS. Sample preparation to arrest hydration was carried out by a modification of the freeze-drying technique described by Orr (7). A small fragment fractured from the paste was carefully placed in a bath of dry pentane cooled to about -125°C. After 2-3 min in the bath, the specimen was carefully removed with tweezers and placed in a vacuum freeze-drying apparatus to remove all free water (8). After about 10 h the specimens were removed and fractured to expose a fresh surface which was mounted and gold-coated for SEM examination. Representative scanning electron micrographs of the hydrating pastes are shown in Fig. 3 and 4. Selected area chemical micro-analysis (EDXA) was used to assist in the identification of microstructural features.

RESULTS AND DISCUSSION

SLAG CHARACTERISTICS

The electrozone particle size analysis data (Fig. 1) are consistent with the Blaine specific surfaces of the slags in showing trends to progressively finer distribution of particle sizes which parallel increasing specific surface. In addition to the particle size statistics, it is interesting to note the percentages by volume of ultrafine particles less than 5 µm, i.e., in the 4000 cm^2/g material, 15.1; in the 5000 cm^2/g, 23.8 v/v. This is likely to be an important observation in assessing the relative chemical reactivity of the slags since the ultrafine particles have high surface area and contribute large part of the activity of the materials, particularly in the early stages of hydration.

The general uniformity of the two slag grades is confirmed by the similarities of specific gravity, in the range of 2.86 to 2.88, as well as by the results of the chemical analysis (Table 3). Chemically, it is interesting to note that the Mg content of the slag is around 18.5% and comparable with levels reported for South African slags (9,10). Calculated hydraulic indices ($CaO+MgO+Al_2O_3/SiO_2$) incorporating the magnesium are approximately 1.6 and are well in excess of the >1.0 requirement of CSA A363-M1977.

Numeralogically (Fig. 5), the slags are predominantly glassy with melilite identified as the minor crystalline phase. In the absence of other observable crystalline phases, it must be concluded that the Mg is distributed between the melilite and the glass, rather than being present as periclase (MgO). This interpretation is consistent with the location of the slag composition in the idealized $CaO-SiO_2-MgO$ ternary system, at 10% Al_2O_3, in the melilite phase field (Fig. 6). In this way, it is useful to consider the new slag as a calcium magnesium aluminosilicate glass in which the Mg is a glass modifying element with a similar function to Ca. In this respect, it has been reported that the Mg^{2+} ion in a glassy slag is present in the fourfold coordination state (11,12).

As noted above, XRD indicates that the slags are predominantly glassy. This was confirmed by the QXRD method using an internal CaF_2 reference and melilite calibration curves (2), from which a melilite content close to 10% w/w was determined for the two slags. With no other discernible phases, by difference, this places the glass content of the materials close to 90% w/w.

A preliminary indication of the strength gain of OPC-BFS (50:50) mortars is shown by comparison with a reference OPC mortar in Table 4. After 7 d curing, all the slag mortars had strengths below the reference. After 28 d curing, however, the OPC-BFS mortars showed a departure from this trend: both 4000 and 5000 cm^2/g slags exceeded the strength of the reference by 101 and 110%, respectively. The air contents of the slag mortars (Table 5) are slightly less than the control mortar and decrease in the increasing slag fineness. According to ASTM C 989-82 definitions, the 4000 and 5000 cm^2/g slags would qualify as "Grade 80" on the basis of their low 7 d strengths, however their 28 d strengths are equivalent to "Grade 100" and "Grade 120", respectively.

PORTLAND CEMENT-SLAG HYDRATION

Pore Fluid Chemistry

The dominant ions present in the pore fluids expressed from both the OPC and OPC-BFS pastes are Ca^{2+}, Na^+, K^+, SO_4^{2-} and OH^-; the concentrations of Si, Fe, Al are very low and close to experimental detection limits (Tables 6

and 7)*. Variations in the concentrations of the dominant ions in solution for all pastes are compared graphically in Fig. 8 as a function of curing age. Similar plots for the data normalized to the initial volume of water are shown in Fig. 8. Trends in these data are noted as follows:

Calcium: calcium levels in the pore fluids are low but there are marked differences between the control and the OPC-BFS pastes. The control reaches a maximum Ca^{2+} level of 4 mmol/L (0.004M) at 3 d, dropping slightly to around 3 mmol/L at 28 d. By comparison, the OPC-BFS pastes exhibit an early Ca^{2+} concentration spike at 2-5 h, this being most noticeable at 70% slag replacement, particularly for the 4000 cm^2/g slag where a Ca^{2+} level of 10 mmol/L (0.01M) was observed at 2 h; the early spike is less pronounced as the fineness of the slag increases. The 28 d Ca^{2+} levels for the OPC-BFS pastes are similar to the control; however, these pastes have lower Ca^{2+} levels than the control at 3 d. These observations are likely associated with differences in the rate of ettringite ($C_3A\bar{S}_3H_{32}$) formation in the pastes, which are controlled by the rate of calcium release by the portland cement and slag. It is thought likely that the 2 h Ca^{2+} spike is not observed in the OPC control due to a greater rate of reaction and that analysis of pore fluids at an earlier age, i.e., less than 1h, would reveal a similar effect. The apparent fall off in Ca^{2+} levels at 2-5 h with increasing slag fineness is consistent with Ca^{2+} release being the dominant factor: a greater rate of Ca^{2+} release would be expected from the finer, higher surface area slag.

Sulphate: Sulphate, originating from the gypsum set regulator added to the clinker, is present in significant concentrations in solution at early ages but is rapidly removed from the system by the formation of highly insoluble ettringite. In general, the SO_4^{2-} levels are in accordance with a simple dilution of the sulphate available from the OPC by slag; thus, while the control shows a maximum sulphate level of 75 mmol/L at 5 h, the OPC-BFS(50:50) pastes exhibit levels of about 35 mmol/L. There appears to be some difference in the rate of sulphate removal from solution, the slag pastes showing much lower relative sulphate levels at 1 d compared to the control. This is likely

---

*Analysis of OPC-BFS (50:50) pastes also indicated that Mg is present in the pore fluid in only trace concentration, close to the detection limits.

related to the higher calcium levels in the slag systems noted above. In the OPC-BFS pastes, there is a small but noticeable increase in the solution sulphate of longer curing age. Three, 7 and 28 d concentrations are 0.6, 1.1 and 7.1 mmol/L, respectively. To some extent this correlates with a small increase in the Ca^{2+} levels in the mature OPC-BFS paste fluids. Whether this signifies the potential for further, and possibly disruptive ettringite formation requires further investigation.

Sodium and potassium: Both sodium and potassium show monotonic increases in concentration in the control paste reaching about 250 mmol/L (0.25 M) at 28 d (Fig. 7). However, when normalized to the initial volume of water (Fig. 8), it is evident that Na^+ reaches steady state after 3 d, while K^+ is essentially at its final level after only 2 h. These observations indicate:

1) that Na^+ and K^+ are not actively involved in the gel formation reactions,
2) that K^+ is associated with OPC phases such as C_3A, which hydrate faster than those rich in Na^+. In general, the Na^+ and K^+ levels in the OPC-BFS pastes conform to the same trends as the control at reduced levels, suggesting that these ions are not released significantly by the hydrating slag. This is some indication, however, that Na^+ and K^+ are removed from solution at 28 d, this being most marked for the finer grade of slag.

Hydroxil and pH: Even at 2 h curing, the pore fluids are substantially alkaline with pH>13. (OH^->100 mmol/L). The control exhibits a monotonic increase in OH^- concentration with curing age to about 500 mmol/L (0.5 M) at 28 d (Fig. 7). Normalized data (Fig. 8) indicate that pseudo steady state is reached at about 3 d. By comparison, the OH^- level in the OPC-BFS pastes is somewhat lower, reaching about 290 mmol/L (50% slag) and about 200 mmol/L (70% slag), in approximate accordance with OPC replacement factors. All the slag systems show a small decrease in OH^-, corresponding to the Na^+ and K^+ depletion, at the longer curing ages, although this does not appear to be related to slag fineness.

Ionic balance: A useful cross-check of the analytical data comes from the cation:anion ionic ratio which should have a value of 1.00 if all contributing ions in solution have been accounted for and determined correctly. It is evident (Tables 6 and 7) that the ionic balance is generally good for analysis of pore fluids from pastes cured beyond 1 d; however, deviations from balance are found for the 2 and 5 h pastes where, analytically, the anions exceed the cations. Interestingly, the deviations are more pronounced for the OPC-BFS (30:70) pastes, suggesting that the analytical problem might be associated with the slag. In summary, it can be seen that the pore fluids expressed from mature control and OPC-BFS pastes conform closely to, and are best described as, solutions of sodium and potassium hydroxides. In the 1 d old pastes, significant levels of sulphate are present in the pore fluids, with sodium and potassium cations rather than calcium. Steady state concentrations of calcium and silicon in the pore fluid are very low, i.e., approximately 0.003 M and 0.0003 M, respectively. The pore fluid from the OPC-BFS (50:50) pastes has approximately one-half the OH^- concentration of the control OPC paste but in terms of the conventional pH scale, i.e., 13.4 versus 13.7, respectively, the difference is not so obvious.

As pointed out by Diamond (5), the concentrations of ions expressed from pastes are controlled by three mechanisms:

1) dissolution of ions from reacting cement, cement additives, e.g., gypsum or slag;
2) removal of ions from pore solution by incorporation into solid reaction products; and
3) concentration by virtue of water uptake from pore fluid by hydration of cement or slag.

For the slag-cement system under study, it is clear that the slag modifies the cement pore fluid chemistry, largely to alter the rate of calcium and sulphate entry and departure. There appears to be no significant introduction of sodium and potassium from the slag itself; like OH^-, these ions appear at reduced levels in the OPC-BFS fluids in approximate accordance with the cement replacement level, i.e., similar to a filler effect.

Calcium hydroxide and non-evaporable water content of pastes

The variation in the TGA/DTG-derived calcium hydroxide and non-evaporable water contents of the OPC and OPC-BFS pastes with curing age are shown in Fig. 9 and 10.

The $Ca(OH)_2$ contents of the pastes generally reflect the replacement level of OPC with slag; thus, the 50:50 and 30:70 OPC-BFS pastes have $Ca(OH)_2$ contents which are around 55% and 37% of the control, respectively, at 28 d with no observable dependence on slag fineness. It would appear from this data that the hydration of the slags does not significantly supplement the $Ca(OH)_2$ produced by the hydration of the OPC. This is shown more clearly in Tables 10 and 11 where it can be seen that the $Ca(OH)_2$ contents of the OPC-BFS pastes, expressed in g/100 g OPC, are similar to the control beyond 1 d curing. The data also indicate that is some inhibition of early $Ca(OH)_2$ production in the slag cement systems up to 1 d.

By comparison, the non-evaporable water contents clearly demonstrate the hydraulic nature of the slags. This is shown clearly for the 50:50 OPC-BFS pastes which find approximately 80% of the water consumed by the control OPC paste; with no slag hydraulic activity, a value close to 50% of the control would be expected. For the 30:70 pastes at 28 d, it is evident that total hydration is slightly less advanced than the 50:50 OPC-BFS systems in the approximately 72% of the control OPC water bound. However, on the basis of simple mass proportions of OPC to slag, it would appear that the slag binds slightly more water at the higher 30:70 replacement level.

From the preceeding data, it is apparent that, compared to the OPC control, the OPC-BFS pastes bind proportionally more water than they liberate $Ca(OH)_2$. Whether the slags are net consumers of $Ca(OH)_2$ is not clear from the present short-term data.

Phase identification and microstructure of pastes

The principal phases identified by XRD in the hydration of the 50:50 OPC-BFS system are shown in Fig. 2. The hydration of the OPC component is shown clearly by the decline of the C_3S and C_2S maxima as $Ca(OH)_2$ and C-S-H gel form. There is some decrease in the intensity of the broad glassy diffraction maxima of the slag with curing age but the effect is not marked and indicates that even at 28 d, slag hydration is not very advanced. Ettringite is observable at 1 d and persists to 28 d curing with no apparent conversion

to monosulphate. The broad line, phase X, centred at 11.4° 2θ (7.8Å) has not been positively identified but is seen to increase in intensity with age. This feature is tentatively assigned to hydrotalcite, $Mg_6Al_2CO_3(OH)_{16}.4H_2O$ (I_{max},7.69Å), which has been reported (13) in the hydration products of slag cements with a significant Mg content, such as those under study. Other workers have also proposed the formation of magnesium aluminate species, M_4AH_x, in the hydration products of high-Mg slag cements (14). An alternative but less likely assignment of this feature is to the carbonated calcium aluminate phase ($Ca_4Al_2CO_3(OH)_{12}.6H_2O$) ($I_{max}$, 7.6Å).

The general morphology of fracture surfaces of the control and slag-cement pastes at 5 h and 7 d are shown in the accompanying scanning electron micrographs (Fig. 3 and 4). Morphologically, the 5 h pastes are very similar in showing the onset of hydration. In the control (Fig. 3), the cement grains are coated with a fine layer of amorphous-looking C-S-H and ettringite; unreacted gypsum crystals are still observable. The 4000 cm^2/g slag-cement system shows similar early growth of C-S-H gel on cement and slag grains (Fig. 4a); again, gypsum is still evident but ettringite growth does not appear to be as advanced as the control and was not positively confirmed by EDXA.

After 7 d curing, there are more pronounced differences between the control and slag-containing pastes. In the control (Fig. 3b), extensive deposits of angular crystalline portlandite, $Ca(OH)_2$, are present together with a more developed growth of fibrillar C-S-H gel (types I and II); where it is distinguishable from the fibrillar C-S-H, the ettringite appears as delicate needles with high aspect ratio. In the slag-containing pastes (Fig. 4b), and in accordance with the thermal analysis results, the deposits of portlandite, $Ca(OH)_2$, are less abundant than in the control; fibrillar C-S-H shows extensive development on both cement and slag grains, adopting a range of morphologies with a predominance of the type II C-S-H. There is some indication in the fields examined, that the ettringite needles in 4000 cm^2/g slag-cement pastes are more abundant and have a lower aspect ratio, i.e., shorter and thicker, than the control. At 7 d, there are no obvious differences in morphology between the two slag-cement pastes which might be attributed to the different finenesses, both showing hydration products with good pore-filling qualities which are comparable to, or slight exceed, the control.

No direct evidence of magnesium-containing phases was obtained by SEM-EDXA micro-analysis in the 7 d samples examined. In this respect, it is

likely that any magnesium aluminate reaction products such as hydrotalcite, might be localized on the surface of the slag grains and, therefore, possibly obscured from view by SEM by C-S-H gel growth. In support of this view, Tanaka et al (15) have observed magnesium enrichment of inner hydrate layers in hydrated slag grains, suggesting that magnesium migration away from the host site is not favoured.

SUMMARY AND CONCLUSIONS

1. A granulated blast furnace slag, ground to nominal finenesses of 4000, and 5000 cm^2/g, has been characterized by a range of techniques. The slag was highly vitreous, about 90% glass, with a significant magnesium content of 18.6%, and was identified principally as a calcium magnesium alumino-silicate glass with melilite as the minor crystalline component. Free MgO was not detected. The high glass content, determined by QXRD, indicates that the granulation trials were successful.
2. Slag activity indices were determined for the two grade fineness as OPC-BFS mortars (50:50) by the ASTM C 989 method at 7 and 28 d and qualified the slags as "Grade 80" on the basis of their 7 d strengths and "Grade 100" on the basis of their 28 d strengths.
3. From the analysis of expressed pore fluids, it is evident that the rates of mobilization of Ca^{2+} and SO_4^{2-} in the immature OPC-BFS pastes differ from the OPC paste. This may be associated with ettringite formation. In mature pastes, the major ions in solution are Na^+, K^+, and OH^- with concentrations approximately one-half those in the control. The slag itself does not appear to contribute significantly to the pore fluid chemistry at 28 d.
4. As determined by the thermogravimetric technique, it is evident that $Ca(OH)_2$ is not formed to any significant extent by the hydration of the slags up to 28 d, the $Ca(OH)_2$ levels in the OPC-BFS pastes correspond closely to those expected for the OPC alone. However, it is not clear from the present data whether the production and consumption of $Ca(OH)_2$ occur at similar rates during the early hydration of the slag. It would be of obvious interest to examine pastes cured beyond 28 d to probe possible pozzolanic activity in the slag. The TGA/DTG-derived non-evaporable water contents confirm the hydraulic nature of the slags.

5. Phase and microstructural characterization of the slag-cement (50:50) pastes at w/c = 0.5 indicates that:

   a) portlandite, $Ca(OH)_2$, is present in lower concentration that in the control;
   b) Type II C-S-H and ettringite are major hydration products;
   c) ettringite has lower aspect ratio than the control; and
   d) a Mg-containing aluminate, possible a hydrotalcite, may be among the hydration products of the slag.

ACKNOWLEDGEMENTS

This study has been carried out at Ontario Research Foundation under DSS Contract 03SQ-23440-4-9174. The principal investigator was R.T. Hemmings, Ontario Research Foundation. The detailed work statement was prepared by E. Douglas, CANMET, Mineral Processing Laboratories, Energy, Mines and Resources Canada, Ottawa, Ont., 1985.

REFERENCES

1. CSA Standard A363-M1983, Cementitious hydraulic slag, Appendix A "Determination of glass content by the modified McMaster Method".

2. Douglas, E., Mainwaring, P.R. and Hemmings, R.T. "Determination of glass content in fly ashes and slags"; CANMET Report 85-6; Energy, Mines and Resources Canada; 1986.

3. Longuet, P. "La phase liquide de ciment hydrate"; Rev des matériaux 1:35-41; 1973.

4. Barneyback, R.S. and Diamond, S. "Expression and analysis of pore fluids from hardened cement pastes and mortars"; Cement and Concrete Res 11:383-394; 1981.

5. Diamond, S. "Effects of two danish flyashes on alkali contents of pore solutions of cement-flyash pastes"; Cement and Concrete Res 11:383-394; 1981.

6. Douglas, S., Mainwaring, P.R. and Hemmings, R.T. "Pozzolanic properties of Canadian non-ferrous slags"; Proc 2nd Int Conf on the Use of Fly Ash, Silica Fume, Slag and Natural Pozzolans in Concrete; Madrid, Spain; April 1986.

7. Orr, D.M.F. "Application of the scanning electron microscope to the study of the initial hydration of portland cement paste"; Cement and Concrete Res 13:146-148; 1983.

8. Characterization of granulated blast furnace slag for portland cement replacement in concrete. Contract Report DSS File No. 03SQ 230-440-4-9174; January 1986.

9. Stutterheim, N. "Some studies on the quarternary system Ca-Al_2O_3-SiO_2-MgO with particular reference to possibilities of making cement from high magnesia blast furnace slags"; S Afr Ind Chem 6:1-8; June 1952.

10. Stutterheim, N. "Properties and uses of high magnesia portland slag cement concretes"; J Am Conc Inst 31:1027-1045; 1960.

11. Roy, R. "Magnesium in four-fold coordination in glass"; J Am Chem Soc 72:3307; 1950.

12. Roy, R., Chopra, S. and Taneja, C.A. "Coordination state of aluminum, magnesium and manganese ions in synthetic slag glasses"; Int Symp on the Chemistry of Cement; Tokyo; IV:228; 1968.

13. Kuhkle, K. and Ludwig, U. "On the use of foundry sands high in MgO in blast furnace cements"; Sprechsaal fur keramic glass email silikate 105:421-432; 1972.

14. Taneja, C.A., Nastro, A. and Sabatelli, V. "Study of the hydration and hydraulic behaviours of vitreous blast furnace slag in relation to the MgO content"; Il Cemento 74:45-52; 1977.

15. Tanaka, H., Totani, Y. and Saito, Y. "Structure of hydrated glassy blast furnace slag in concrete"; Proc CANMET/ACI 1st Int Conf on the Use of Fly Ash, Silica Fume, Slag and Other Mineral By-products in Concrete; Montebello, Que; In: ACI publication SP-79, V.M. Malhotra, Editor; II:963-977; 1983.

Table 1 - Chemical and physical characteristics of portland cement

Chemical Analysis(%)*		Physical Properties	
SiO_2	21.3	Normal consistency (ASTM C187)	22.8%
Al_2O_3	4.3		
Fe_2O_3	2.3	Vicat set time (ASTM C191)	
MgO	3.6	initial	129 min
CaO	62.8	final	210 min
Na_2O	0.47		
K_2O	0.50	Fineness (ASTM C184,C430)	
SO_3	2.92	- 75 µm	98.7%
CaO (free)	0.02	- 45 µm	91.3%
LOI	1.69		
Insol. residue	0.20	Blaine (ASTM C204)	4070 cm^2/g
Bogue Composition:		Compressive strength of mortar Cubes (ASTM C109):	
C_3S	53.2	1 d	10.7 MPa
C_2S	21.0	3 d	22.0 MPa
C_3A	7.5	7 d	26.9 MPa
C_4AF	7.0	28 d	35.0 MPa
CaO	0.02		
MgO	3.6	Autoclave Expansion	0.09%
$C\bar{S}H_2$	6.3	*ASTM C151)	
Total †	98.6		

* Method ASTM C114; Fe by atomic absorption spectroscopy

† Analysis total including minor oxides, Na_2O and K_2O, insol. residue, and LOI not associated with gypsum = 100.3%.

Table 2 - Specific gravities and particle size analysis of laboratory ground blast furnace slags

Slag, cm^2/g	Specific gravity	Particle size (μm)	
		Mean	Median
4000	2.86	13.2	15.3
5000	2.88	10.5	11.6

Table 3 - Chemical analysis data for slags

Hydraulic Index**	4000 cm^2	5000 cm^2/g
SiO_2	38.1	38.4
Al_2O_3	8.7	8.8
Fe_2O_3	0.35	0.61
CaO	32.6	32.3
MgO	18.7	18.6
Na_2O	0.22	0.22
TiO_2	0.63	0.36
K_2O	0.80	0.71
P_2O_5	<0.01	<0.01
BaO	0.03	0.03
SrO	0.05	0.05
ZrO_2	0.01	0.01
SO_3*	2.80	2.36
LOI	-2.06	02.01
Total	99.22	99.48
Hydraulic Index**	1.58	1.58

* Total sulphur as SO_3

** $CaO + MgO + Al_2O_3/SiO_2$

Table 4 - Slag activity index data for OPC-BFS mortars*

Mortar I.D.	Mix proportions: Cement (gm)	Sand (gm)	Slag (gm)	Water (mL)	Flow value	W/CZ	Age	Compressive strength, psi: I	II	III	Avg.	Slag activity index, %
Reference	500	1375	--	232	107	0.464	7	5288	4938	5063	5096	--
							28	5675	5675	5825	5725	--
4000 cm^2/g	250	1375	250	230	108	0.460	7	3250	2850	3238	3113	61
							28	5825	5675	5850	5783	101
5000 cm^2/g	250	1375	250	230	109	0.460	7	3275	3475	3388	3379	66
							28	6300	6325	6250	6292	110

* According to ASTM C989

† Total binder, i.e., OPC+BFS

Table 5 - Air content of mortars

	Mix proportions						
Mortar I.D.	Cement (gm)	Sand (gm)	Slag (gm)	Water (mL)	Flow value	w/C	Air content %
Reference	350	1400	--	230	86	0.657	11.0
4000 cm^2/g	--	1400	350	230	89	0.657	9.5
5000 cm^2/g	--	1400	350	225	88	0.643	8.6

* According to ASTM C185

Table 6 - Chemical data for pore fluid extracted from slag-cement pastes (50% w/w slag)

Paste	Age	IONIC CONCENTRATIONS (mmol/L)									
		pH	Si	Fe	Ca	Al	Na	K	SO_4^{2-}	OH^-	Cations* / Anions
Control (0% Slag)	2 h	13.11	<0.1	0.01	0.5	<0.1	77	135	69.4	129	0.80
	5 h	13.13	0.4	0.01	0.9	<0.1	82	142	75.5	134	0.79
	1 d	13.36	1.8	<0.01	0.6	<0.1	137	162	48.7	227	0.93
	3 d	13.62	1.7	0.04	4.0	0.1	215	203	5.4	418	0.99
	7 d	13.66	0.9	0.03	2.9	0.1	227	216	3.9	455	0.97
	28 d	13.70	0.6	0.17	3.0	0.1	257	247	4.6	503	1.00
4000(50)	2 h	13.01	0.3	0.01	0.4	<0.1	37	74	33.7	102	0.66
	5 h	12.99	0.3	0.01	1.6	<0.1	40	75	36.2	99	0.69
	1 d	13.25	1.0	0.01	0.8	0.1	78	90	5.9	176	0.90
	3 d	13.39	0.6	0.01	1.0	0.1	113	110	0.6	246	0.91
	7 d	13.45	0.6	0.02	1.1	0.2	128	123	0.7	280	0.90
	28 d	13.45	0.3	0.02	2.8	<0.1	147	127	2,8	285	0.96
5000(50)	2 h	13.02	<0.1	-	0.9	<0.1	36	70	4.8	105	0.94
	5 h	13.02	0.4	-	0.4	0.1	38	70	27.8	104	0.68
	1 d	13.28	1.0	-	0.4	<0.1	82	90	1.8	190	0.89
	3 d	13.41	0.1	-	0.4	0.1	120	122	0.6	255	0.95
	7 d	13.46	0.1	-	3.8	0.1	141	128	0.7	288	0.96
	28 d	13.44	0.3	0.05	2.7	<0.1	147	125	2.1	274	1.00

* Ion balance: $\frac{2\,Ca + Na + K}{2\,SO_4^{2-} + OH^-}$

Table 7 - Chemical data for pore fluid extracted from slag-cement pastes (70% w/w slag)

Paste	Age	IONIC CONCENTRATIONS (mmol/L)									
		pH	Si	Fe	Ca	Al	Na	K	SO_4^{2-}	OH^-	Cations* / Anions
Control (0% Slag)	2 h	13.11	<0.1	0.01	0.5	<0.1	77	135	69.4	129	0.80
	5 h	13.13	0.4	0.02	0.9	<0.1	82	142	75.5	134	0.79
	1 d	13.36	1.8	<0.01	0.6	<0.1	137	162	48.7	227	0.93
	3 d	13.62	1.7	0.04	4.0	0.1	215	203	5.4	418	0.99
	7 d	13.66	0.9	0.03	2.9	0.1	227	216	3.9	455	0.97
	28 d	13.70	0.6	0.17	3.0	0.1	257	247	4.6	503	1.00
4000(70)	2 h	12.92	<0.1	-	10.4	<0.1	21	45	20.0	93	0.71
	5 h	12.96	0.1	-	0.5	<0.1	23	48	17.2	92	0.57
	1 d	13.15	1.5	-	0.4	0.3	60	61	0.6	142	0.85
	3 d	13.24	0.1	-	0.6	0.1	76	77	0.6	175	0.88
	7 d	13.29	<0.1	-	2.9	0.1	89	86	0.7	195	0.92
	28 d	13.25	0.3	0.01	2.3	0.1	84	72	3.6	178	0.87
5000(70)	2 h	12.91	0.1	<0.01	6.0	<0.1	25	41	27.5	81	0.57
	5 h	12.96	0.3	<0.01	3.7	<0.1	24	46	25.6	92	0.54
	1 d	13.17	0.2	<0.01	0.5	<0.1	56	67	0.8	148	0.83
	3 d	13.27	0.1	<0.01	0.3	0.1	79	81	1.2	188	0.85
	7 d	13.29	0.2	<0.01	0.6	0.1	83	85	1.2	193	0.87
	28 d	13.23	0.2	<0.01	3.0	0.1	80	59	3.5	170	0.82

* Ion balance: $\frac{2\,Ca + Na + K}{2\,SO_4^{2-} + OH^-}$

Table 8 - Chemical data for pore fluid normalized to initial volume of water (50% w/w slag)

Paste	Age	IONIC CONCENTRATIONS (mmol/L)								
		pH	Si	Fe	Ca	Al	Na	K	SO_4^{2-}	OH^-
Control (0% Slag)	2 h	13.10	<0.1	0.01	0.5	<0.1	74	130	67.1	125
	5 h	13.10	0.4	<0.01	0.8	<0.1	77	133	70.9	126
	1 d	13.23	1.3	<0.01	0.4	<0.1	102	120	36.2	169
	3 d	13.41	1.1	0.02	2.5	0.1	133	125	3.3	259
	7 d	13.42	0.5	0.02	1.8	0.1	130	124	2.2	261
	28 d	13.41	0.3	0.09	1.5	0.1	131	126	2.3	256
4000(50)	2 h	13.00	<0.1	0.01	0.4	<0.1	36	73	33.2	101
	5 h	12.98	0.4	0.01	1.6	<0.1	39	73	35.3	96
	1 d	13.17	1.3	0.01	0.7	0.1	66	87	5.0	150
	3 d	13.27	1.1	0.01	0.8	0.1	86	84	0.5	188
	7 d	13.28	0.5	0.01	0.8	0.1	88	85	0.5	193
	28 d	13.23	0.3	0.01	1.7	<0.1	88	76	1.7	171
5000(50)	2 h	13.01	<0.1	-	0.9	<0.1	35	68	4.7	103
	5 h	13.00	0.4	-	0.4	0.1	37	68	26.9	101
	1 d	13.20	0.1	-	0.3	<0.1	69	76	1.5	160
	3 d	13.28	0.1	-	0.3	0.1	90	91	0.4	190
	7 d	13.29	0.1	-	2.6	0.1	96	87	0.5	196
	28 d	13.20	0.2	0.03	1.6	<0.1	86	73	1.2	160

Table 9 - Chemical data for pore fluid normalized to initial volume of water (50% w/w slag)

Paste	Age	IONIC CONCENTRATIONS (mmol/L)								
		pH	Si	Fe	Ca	Al	Na	K	SO_4^{2-}	OH^-
Control (0% Slag)	2 h	13.10	<0.1	0.01	0.5	<0.1	74	130	67.1	125
	5 h	13.10	0.4	<0.01	0.8	<0.1	77	133	70.9	126
	1 d	13.23	1.3	<0.01	0.4	<0.1	102	120	36.2	169
	3 d	13.41	1.1	0.02	2.5	0.1	133	125	3.3	259
	7 d	13.42	0.5	0.02	1.7	0.1	130	124	2.2	261
	28 d	13.41	0.3	0.09	1.5	0.1	131	126	2.3	256
4000(70)	2 h	12.91	<0.3	-	10.3	<0.1	21	45	19.8	82
	5 h	12.96	0.1	-	0.5	<0.1	23	47	16.9	91
	1 d	13.12	0.4	-	0.4	0.3	54	55	0.5	133
	3 d	13.20	0.1	-	0.5	0.1	64	64	0.5	157
	7 d	13.17	0.2	-	2.2	0.1	69	67	0.5	149
	28 d	13.08	0.1	0.01	1.5	0.1	56	48	2.4	119
5000(70)	2 h	12.90	0.1	<0.01	5.9	<0.1	25	41	27.3	80
	5 h	12.96	0.3	<0.01	3.7	<0.1	24	46	25.3	91
	1 d	13.12	0.2	<0.01	0.4	<0.1	50	59	0.7	131
	3 d	13.19	0.1	<0.01	0.2	0.1	65	66	1.0	154
	7 d	13.16	0.2	<0.01	0.5	0.1	63	64	0.9	146
	28 d	13.04	0.1	<0.01	2.0	0.1	53	42	1.3	111

Table 10 - TGA/DTG Data for OPC-BFS pastes (50% replacement)

		$Ca(OH)_2$ content		Bound water content	
		per 100 g	per 100 g	per 100 g	per 100 g
Paste	Age	Total binder	OPC	Total binder	OPC
Control	2 h	1.50	1.50	1.67	1.67
(0% Slag)	5 h	2.69	2.69	3.03	3.03
	1 d	14.30	14.30	12.88	12.88
	3 d	20.46	20.46	19.02	19.02
	7 d	24.19	24.19	21.30	21.30
	28 d	26.50	26.50	24.51	24.51
4000(50)	2 h	0.22	0.44	0.72	1.44
	5 h	0.65	1.30	1.27	2.54
	1 d	7.31	14.62	7.52	15.05
	3 d	10.67	21.13	11.86	23.72
	7 d	12.77	25.53	15.58	31.15
	28 d	14.23	28.46	20.05	40.10
5000(50)	2 h	0.39	0.78	1.08	2.16
	5 h	0.72	1.45	1.57	3.14
	1 d	7.02	14.03	7.85	15.70
	3 d	10.71	21.42	12.66	25.32
	7 d	12.27	24.54	16.02	32.05
	28 d	14.62	29.24	20.84	41.67

Table 11 - TGA/DTG Data for OPC-BFS pastes (70% replacement)

Paste	Age	$Ca(OH)_2$ content per 100 g Total binder	$Ca(OH)_2$ content per 100 g OPC	Bound water content per 100 g Total binder	Bound water content per 100 g OPC
Control	2 h	1.50	1.50	1.67	1.67
(0% Slag)	5 h	2.69	2.69	3.03	3.03
	1 d	14.30	14.30	12.88	12.88
	3 d	20.46	20.46	19.02	19.02
	7 d	24.19	24.19	21.30	21.30
	28 d	26.50	26.50	24.51	24.51
4000(70)	2 h	0.0	0.0	0.47	1.57
	5 h	0.17	0.57	0.76	2.53
	1 d	4.14	14.70	5.20	17.32
	3 d	6.14	20.47	8.15	27.16
	7 d	8.31	27.70	11.28	37.60
	28 d	9.93	33.09	16.61	55.37
5000(70)	2 h	0.34	1.12	0.43	1.44
	5 h	0.38	1.27	0.57	1.91
	1 d	4.16	13.87	5.63	18.77
	3 d	5.80	19.34	9.01	30.04
	7 d	7.59	25.30	12.27	40.90
	28 d	9.70	32.33	17.49	58.29

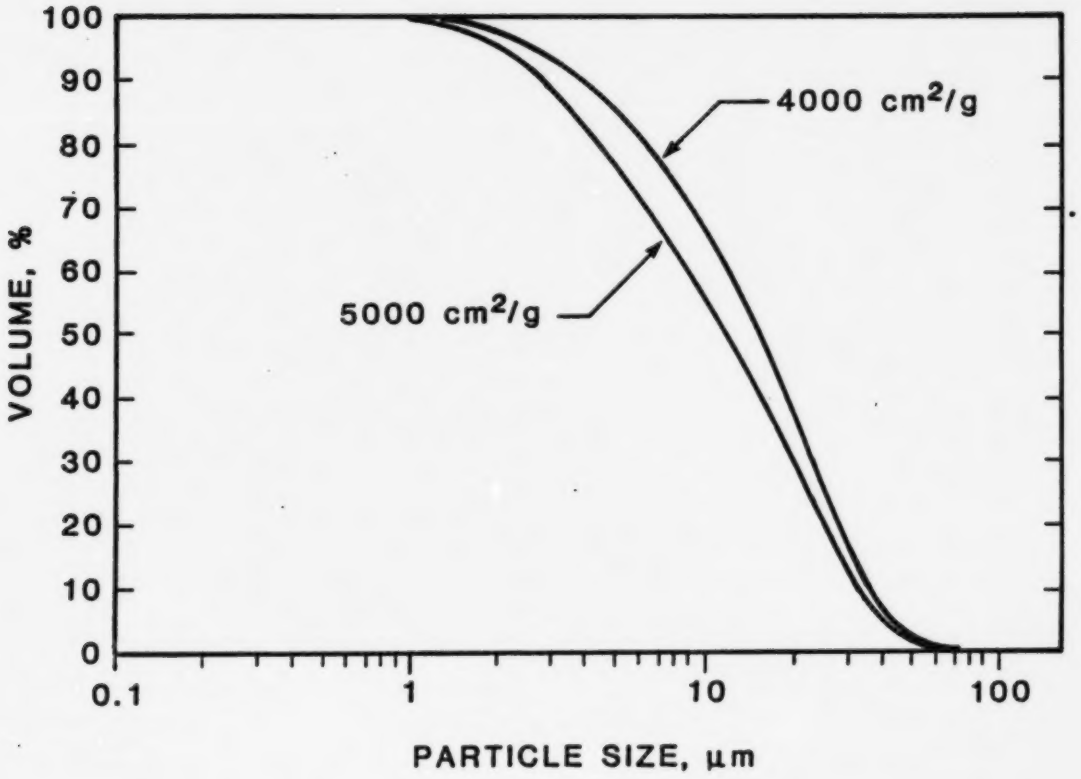

Figure 1. Particle size distribution of 4000 and 5000 cm^2/g slags.

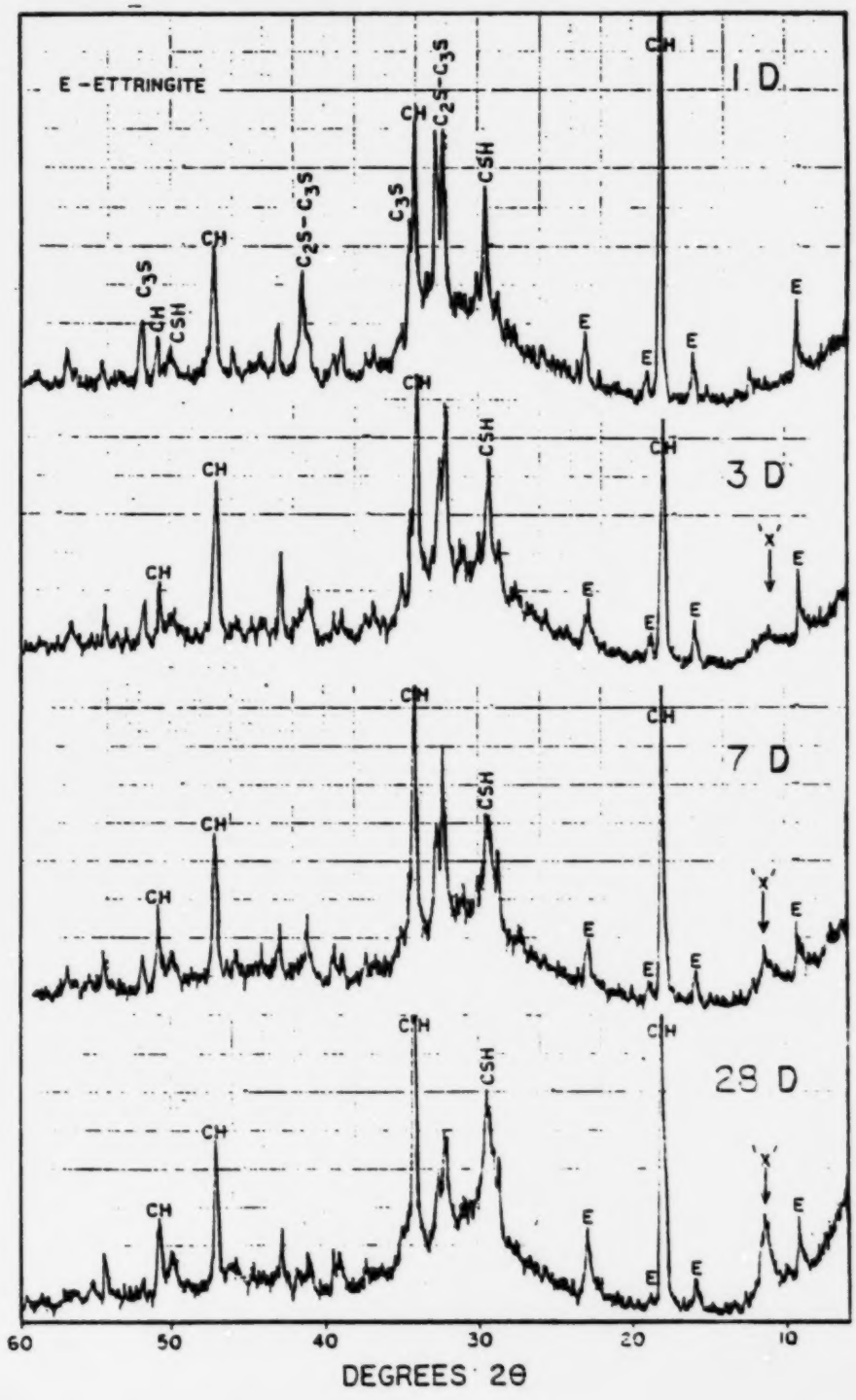

FIGURE 2. XRD Traces showing identification of principal phases in OPC-BFS pastes (50:50)
Phase "x" is tentatively assigned as Hydrotalcite (see text).

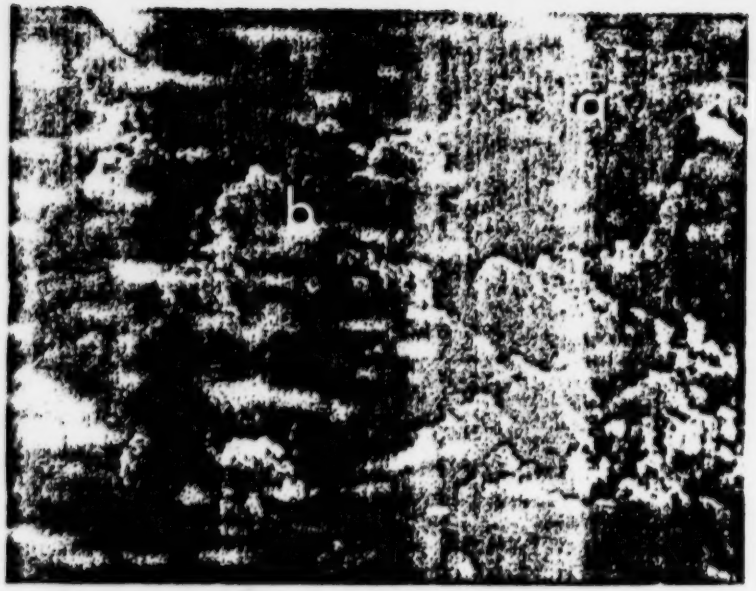

FIGURE 3a. Scanning electron micrographs of control OPC paste at 5h (w/c - 0.5):

a. early stage C-S-H growth

b. ettringite(?)

c. calcium hydroxide

d. gypsum needle

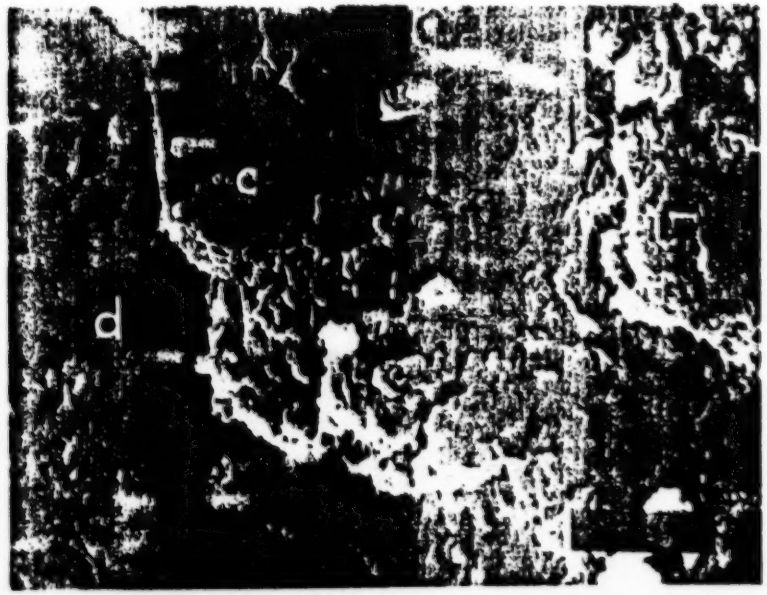

FIGURE 3b. Scanning electron micrographs of OPC control paste at 7d (w/c = 0.5):

a. fibrillar C-S-H (type II?)

b. ettringite (high aspect ratio)

c. calcium hydroxide

d. pore space

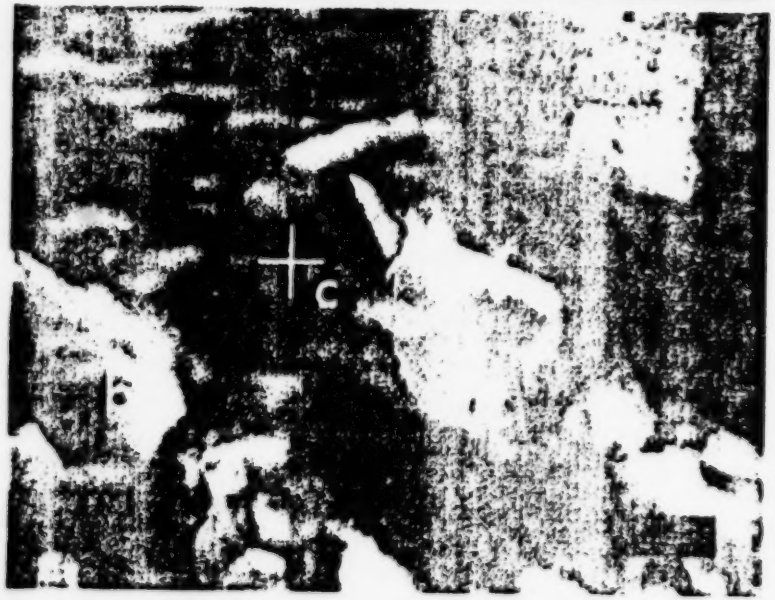

FIGURE **4a.** Scanning electron micrographs of 4000 cm^2/g slag cement paste at 5h (w/c = 0.5):

a. early growth of C-S-H and ettringite(?)

b. slag grain, unhydrated

c. gypsum

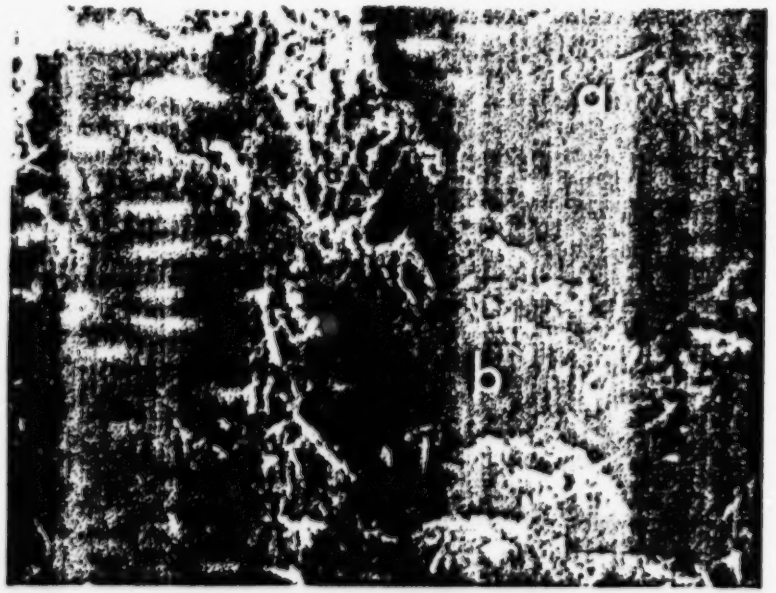

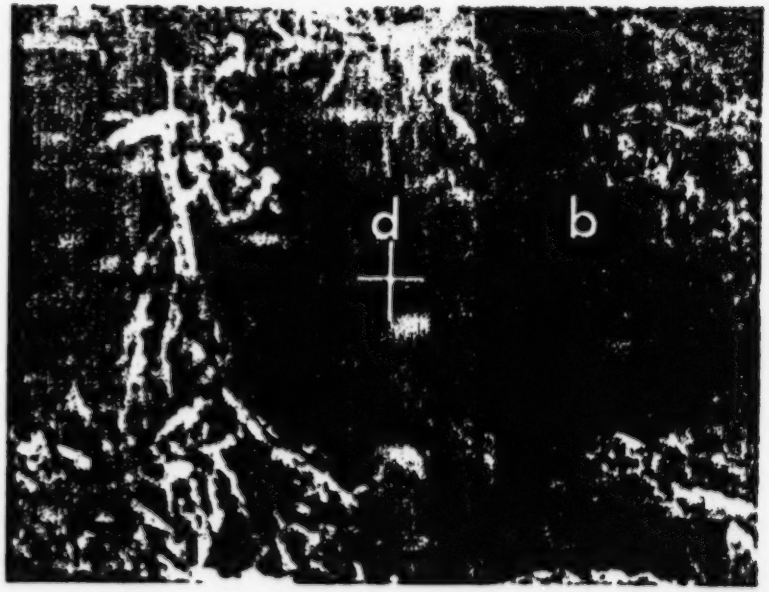

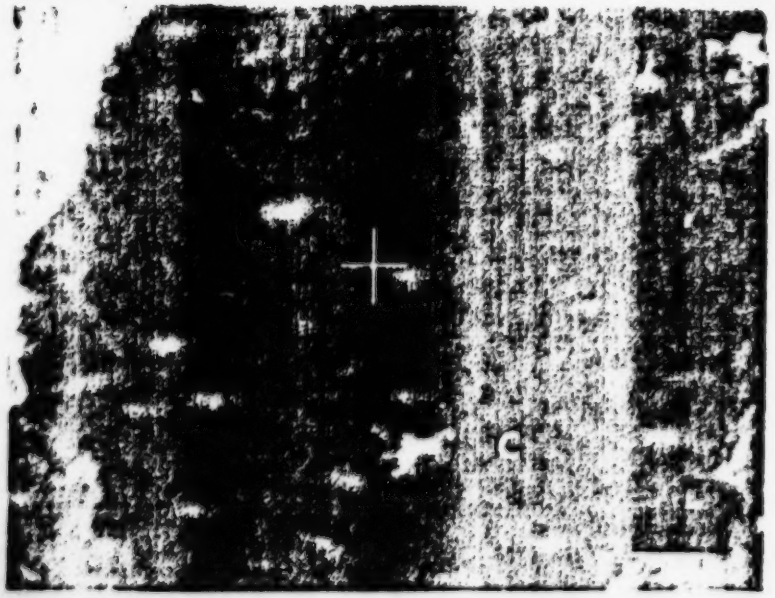

FIGURE 4b. Scanning electron micrographs of 4000 cm^2/g slag-cement paste at 7d (w/c = 0.5):

a. C-S-H (type II)
b. ettringite (low aspect ratio)
c. calcium hydroxide
d. unreacted surface of slag grain

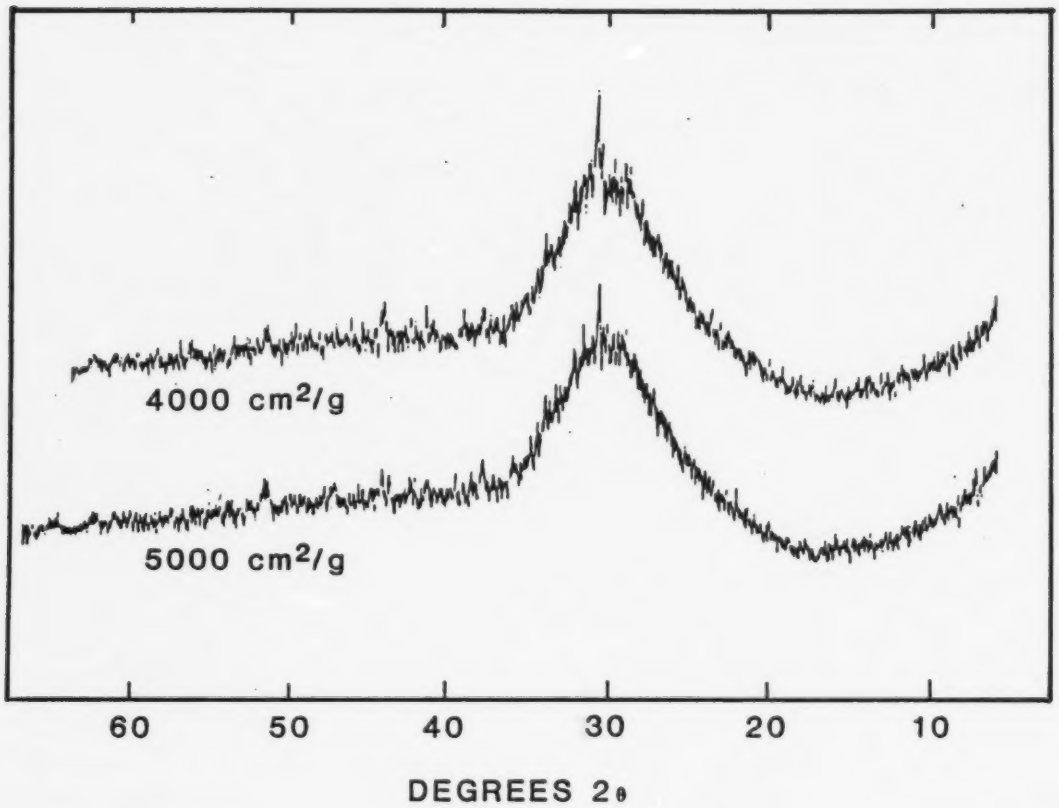

Figure 5. XRD traces (CuK_α) for slags.

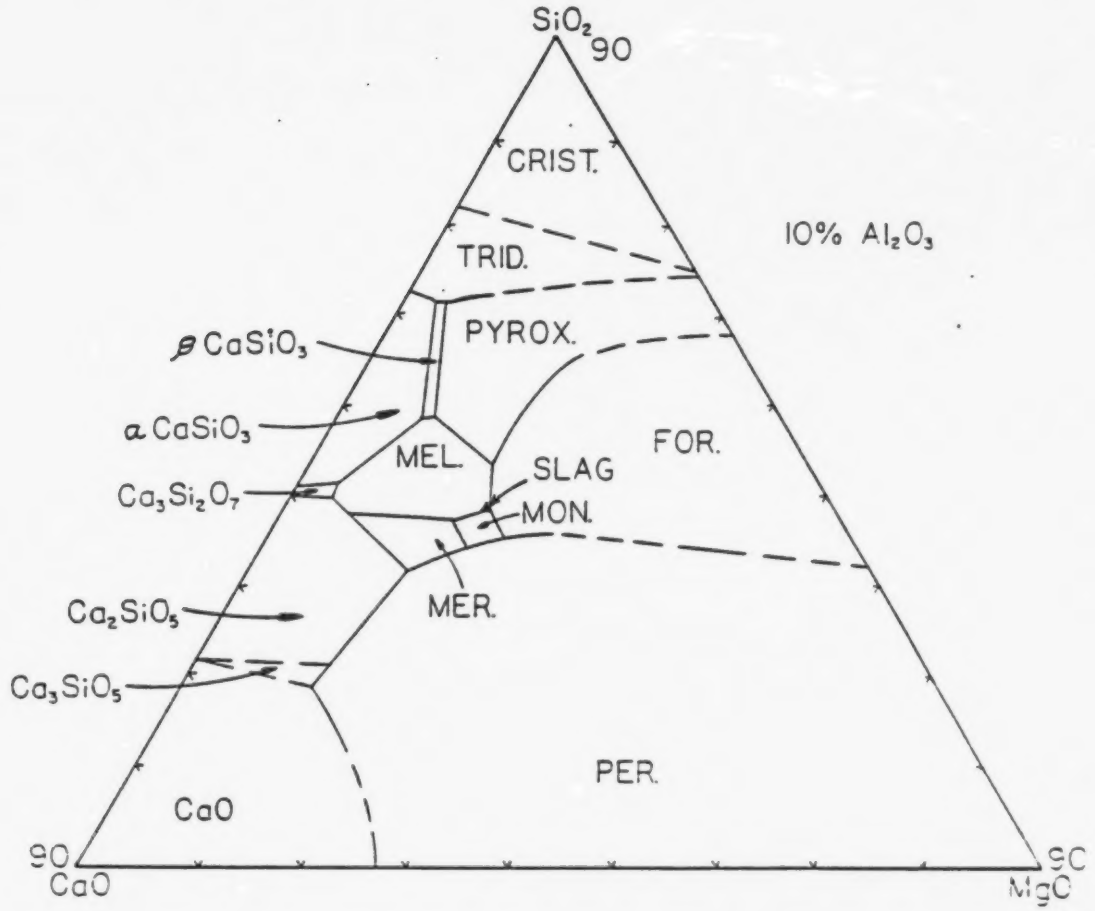

FIGURE 6. Location of Slag Composition in idealized $CaO-SiO_2-MgO$ phase system ($10\%\ Al_2O_3$)

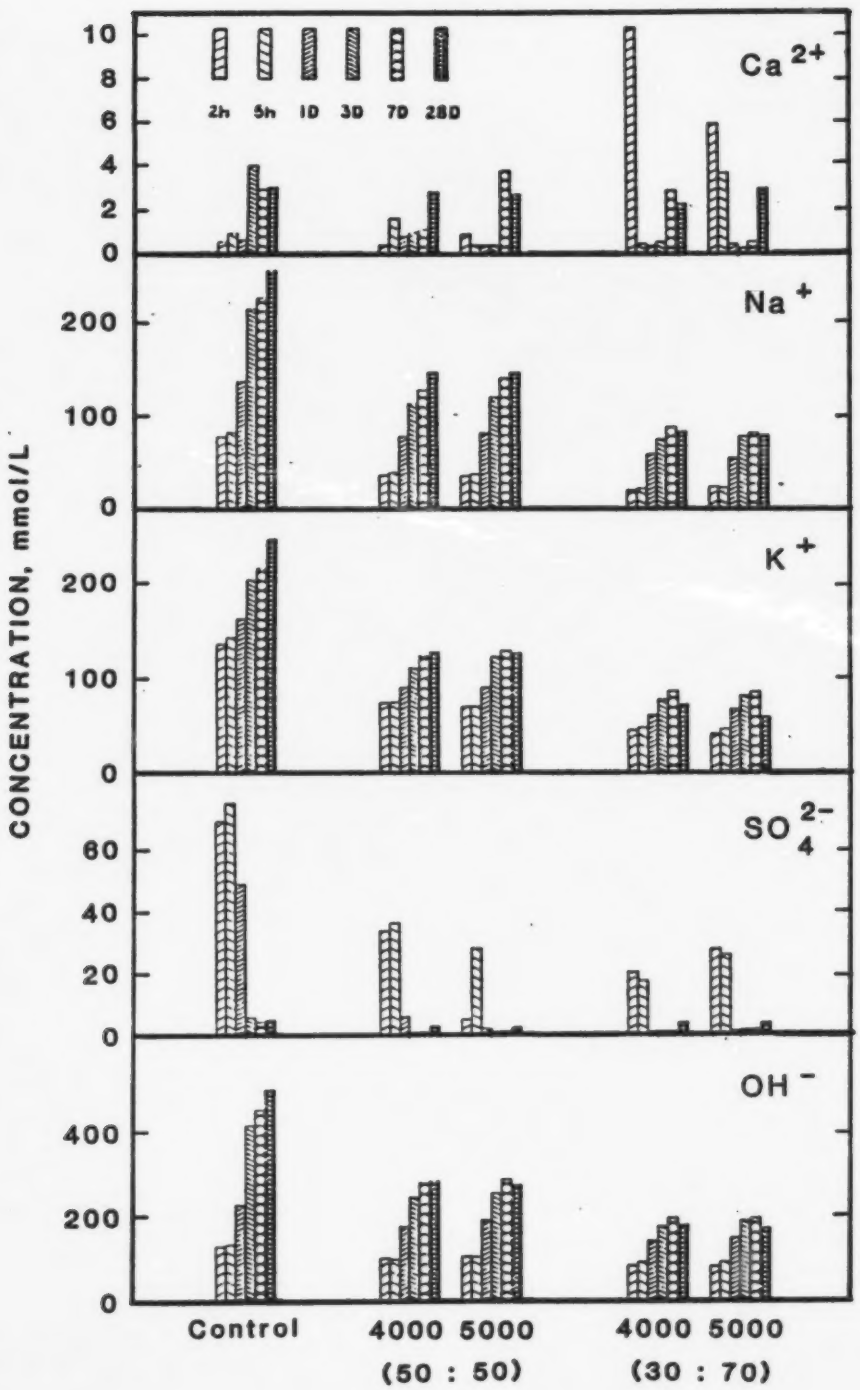

Figure 7. Uncorrected variation in concentration of principal pore fluid ions expressed from OPC-BFS pastes (50:50 and 30:70) at curing ages up to 28 days.

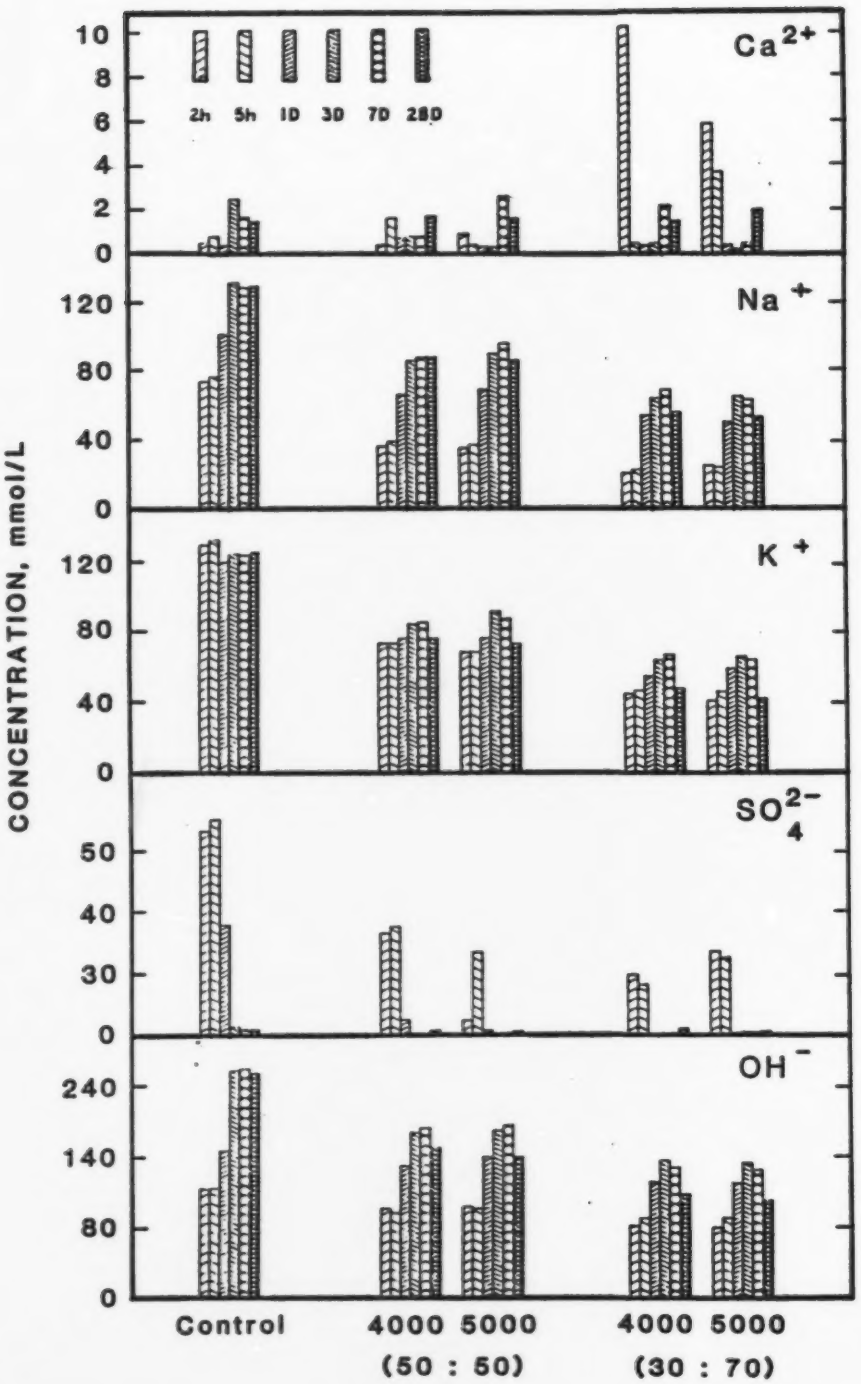

Figure 8. Variation in concentration of principal pore fluid ions expressed from OPC-BFS pastes (50:50 and 30:70) at curing ages up to 28 days (data normalized to initial H_2O volume).

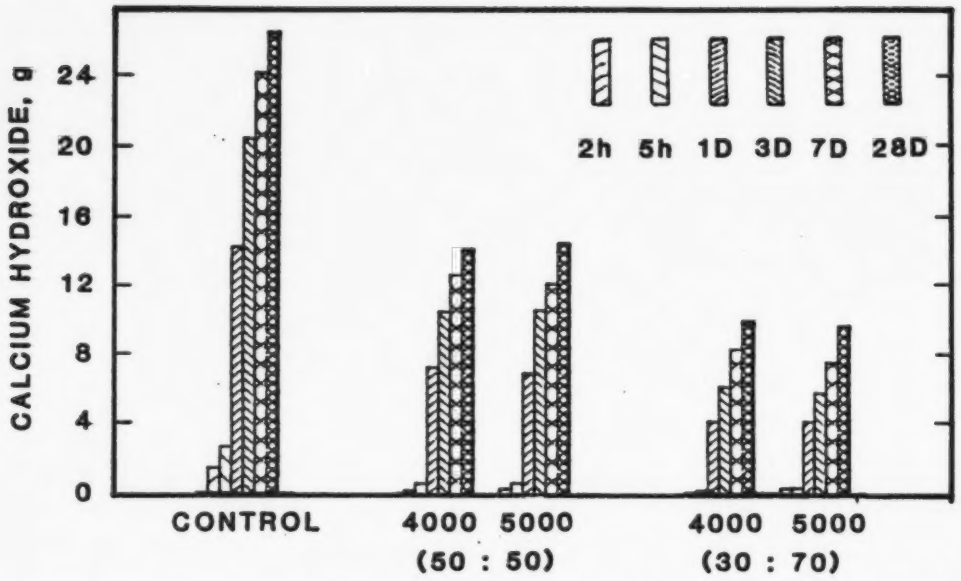

Figure 9. Calcium hydroxide content of portland cement-slag pastes in g/100 total binder.

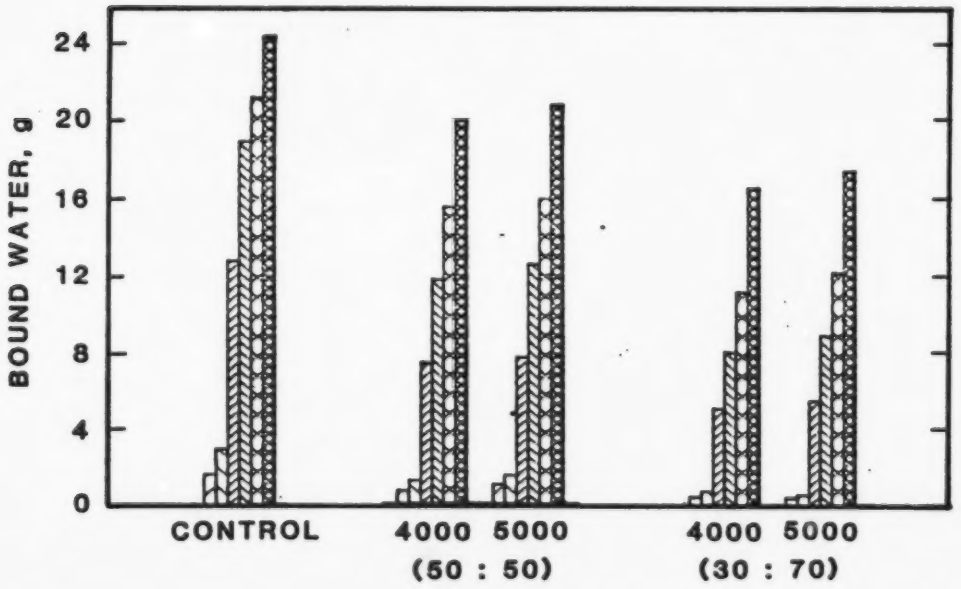

Figure 10. Non-evaporable water content in g/100 total binder, of portland cement-slag pastes.